Transforming growth factor-β1 modulates the expression of vascular endothelial growth factor by osteoblasts

PIERRE B. SAADEH,[1] BABAK J. MEHRARA,[2] DOUGLAS S. STEINBRECH,[2] MATTHEW E. DUDZIAK,[2] JOSHUA A. GREENWALD,[2] JONATHAN S. LUCHS,[2] JASON A. SPECTOR,[2] HIKARU UENO,[3] GEORGE K. GITTES,[2] AND MICHAEL T. LONGAKER[2]

[1]*Department of Surgery, University of Connecticut, Farmington, Connecticut 06032;* [2]*Laboratory of Developmental Biology and Repair, Department of Surgery, New York University School of Medicine, New York, New York 10016; and* [3]*Department of Cardiology, Kyushu University School of Medicine, Fukuoka 812, Japan*

Saadeh, Pierre B., Babak J. Mehrara, Douglas S. Steinbrech, Matthew E. Dudziak, Joshua A. Greenwald, Jonathan S. Luchs, Jason A. Spector, Hikaru Ueno, George K. Gittes, and Michael T. Longaker. Transforming growth factor-β1 modulates the expression of vascular endothelial growth factor by osteoblasts. *Am. J. Physiol.* 277 (*Cell Physiol.* 46): C628–C637, 1999.—Angiogenesis is essential to both normal and pathological bone physiology. Vascular endothelial growth factor (VEGF) has been implicated in angiogenesis, whereas transforming growth factor-β1 (TGF-β1) modulates bone differentiation, matrix formation, and cytokine expression. The purpose of this study was to investigate the relationship between TGF-β1 and VEGF expression in osteoblasts and osteoblast-like cells. Northern blot analysis revealed an early peak of VEGF mRNA (6-fold at 3 h) in fetal rat calvarial cells and MC3T3-E1 osteoblast-like cells after stimulation with TGF-β1 (2.5 ng/ml). The stability of VEGF mRNA in MC3T3-E1 cells was not increased after TGF-β1 treatment. Actinomycin D inhibited the TGF-β1-induced peak in VEGF mRNA, whereas cycloheximide did not. Blockade of TGF-β1 signal transduction via a dominant-negative receptor II adenovirus significantly decreased TGF-β1 induction of VEGF mRNA. Additionally, TGF-β1 induced a dose-dependent increase in VEGF protein expression by MC3T3-E1 cells ($P < 0.01$). Dexamethasone similarly inhibited VEGF protein expression. Both TGF-β1 mRNA and VEGF mRNA were concurrently present in rat membranous bone, and both followed similar patterns of expression during rat mandibular fracture healing (mRNA and protein). In summary, TGF-β1-induced VEGF expression by osteoblasts and osteoblast-like cells is a dose-dependent event that may be intimately related to bone development and fracture healing.

angiogenesis; bone; fracture

NORMAL AND PATHOLOGICAL BONE physiology is inexorably tied to angiogenesis. The process of bone development and repair depends on the adequate formation of new capillaries from existing blood vessels (37). The osteon forms around a haversian canal containing blood vessels that supply osteoblasts with needed oxygen and nutrients. During both intramembranous and endochondral ossification, bone spicules and osteogenic buds, respectively, delineate and surround capillaries. Additionally, osteocyte survival requires a <0.1-mm proximity to nutrient vessels (17), and interruption of the blood supply to bone results in avascular necrosis (9). Furthermore, vascularized bone grafts maintain more osseous mass than nonvascularized bone grafts (10).

As molecular mechanisms of angiogenesis become defined, cytokines and their interrelationships appear to play a crucial role in the formation, growth, and regression of blood vessels. Vascular endothelial growth factor (VEGF), a dimeric heparin-binding glycoprotein, is assuming an increasingly central role in the understanding of the development and modulation of angiogenesis. VEGF is expressed in highly vascular tissues and is an endothelial cell-specific mitogen (23). VEGF receptor knockout mice lack adequate blood vessel formation (34), whereas loss of a single VEGF allele is lethal in the mouse embryo (12). Devascularized rat islets of Langerhans cells and hypoxic human vascular smooth muscle cells demonstrate increased VEGF expression (5).

Fracture healing requires adequate angiogenesis, and it is within this context that VEGF may also play an important role. VEGF is expressed in the normal rat tibia (19), whereas both intramembranous and endochondral ossification is associated with capillary development (8). Additionally, VEGF expression in osteoblasts and osteoblast-like cells is increased by several cytokines and growth factors, including prostaglandin E_1 (PGE_1) and PGE_2, insulin-like growth factor (IGF), platelet-derived growth factor, and 1α,25-dihydroxyvitamin D_3 (14, 19, 38).

Transforming growth factor-β1 (TGF-β1), a ubiquitous cytokine with wide-ranging effects, has been implicated in osteoblast proliferation and differentiation. Moreover, TGF-β1, the largest source of which is bone (3), is expressed at high levels during bone growth and development (25, 33), processes that depend on an adequate blood supply. The observation that TGF-β1 is both a potent inducer and a potent inhibitor of angiogenesis has given rise to the concept that, to promote angiogenesis, TGF-β1 requires an inflammatory environment (28). It is within this inflammatory "context" that TGF-β1 is then able to effect an angiogenic cascade. Support for this concept of "indirect" angiogenesis is provided by the observation that TGF-β1 increases VEGF production in human smooth muscle cells, mouse

The costs of publication of this article were defrayed in part by the payment of page charges. The article must therefore be hereby marked "*advertisement*" in accordance with 18 U.S.C. Section 1734 solely to indicate this fact.

0363-6143/99 $5.00 Copyright © 1999 the American Physiological Society

fibroblasts, human lung adenocarcinoma cells, and human histiocytic lymphoma cells (28).

An increasing body of evidence implicates TGF-β1 in fracture healing. TGF-β1 stimulates osteoblast migration, modulates osteoblast proliferation, and is localized to cells within the developing skeleton (11, 29). Additionally, TGF-β1 expression is increased in fracture healing (21), and exogenous application of TGF-β1 accelerates both endochondral bone fracture healing and the closure of membranous bone critical size defects (2, 24). Despite the above findings, the relationship between TGF-β1 and VEGF in bone growth and healing remains undefined.

Given the importance of TGF-β1 and VEGF in the related processes of angiogenesis and fracture healing, we proposed that TGF-β1 may regulate VEGF expression in osteoblasts. We demonstrated that TGF-β1 increased VEGF mRNA in both primary and clonal osteoblasts. Significant control of this mechanism occurred at the transcriptional level in clonal osteoblasts. Overexpression of a dominant-negative receptor II by adenovirus-mediated gene transfer disrupted TGF-β1 signal transduction and significantly decreased stimulation of VEGF mRNA by exogenous TGF-β1. Additionally, TGF-β1 increased VEGF protein production by osteoblastic cells, and this increase was inhibited by dexamethasone. Finally, synchronously modulating levels of both TGF-β1 and VEGF mRNA and protein expression were found during membranous bone fracture healing.

MATERIALS AND METHODS

Materials. Tissue culture plates and flasks were purchased from Fisher Scientific (Pittsburgh, PA). DMEM, α-modified Eagle's medium, 0.05% trypsin-EDTA, PBS, fetal bovine serum (FBS), and cell culture reagents were purchased from Life Technologies (Gaithersburg, MD). Recombinant human TGF-β1 (Life Technologies) was prepared in 100 ng/5 ml PBS aliquots and was stored at −20°C. Actinomycin D, cycloheximide, and dexamethasone were from Sigma (St. Louis, MO).

Cell culture. Fetal rat calvarial (FRC) cells were cultured from FRC explants by a modification of the procedure described by Freshney (13). Briefly, frontal and parietal bones from gestational 21-day Sprague-Dawley fetal rats were sterilely stripped of their periosteum and minced into 1-mm^3 fragments. The explants were washed with sterile PBS containing an antibiotic and antimycotic and then placed at the bottom of an upright 25-cm^2 flask containing preincubated media (DMEM supplemented with 10% FBS, 100 μg/ml penicillin G, 50 μg/ml streptomycin, and 0.25 μg/ml amphotericin B). After 15 min at 37°C, the flask was slowly returned to a horizontal position, and the culture was maintained in a humidified atmosphere consisting of 95% air-5% CO_2 at 37°C. Media were changed, and when the cells were confluent, the explant pieces were removed and the cells were trypsinized and transferred to 75-cm^2 flasks. *Passage 2* cells were used for all experiments. Verification of osteoblastic lineage was performed by mineralized bone nodule formation assay and Northern analysis for osteocalcin (data not shown).

MC3T3-E1 cells, a mouse clonal osteoblastic cell line, were grown in DMEM supplemented with 10% FBS, 100 μg/ml penicillin G, 50 μg/ml streptomycin, and 0.25 μg/ml amphotericin B. Media were changed every 2–3 days. Confluent MC3T3-E1 cell cultures were trypsinized with 0.05% trypsin and replated in a 1:2 ratio. All cultures were maintained in a humidified atmosphere consisting of 95% air-5% CO_2 at 37°C.

Animals. Adult male Sprague-Dawley rats (250–350 g) were purchased from Taconic Laboratories (Germantown, NY) and housed in separate cages. Animals were kept under a constant 12-h light-dark schedule and fed Purina rodent chow ad libitum. Surgical procedures were approved by the Institutional Care and Use Committee at New York University Medical Center. Anesthesia for all operative procedures was achieved with a mixture of Ketaset (7.5 mg/kg body wt; Fort Dodge Animal Health, Fort Dodge, IA), xylazine (1.5 mg/kg; Bayer Animal Health, Shawnee Mission, KS), and acepromazine maleate (0.25 mg/kg; Fermenta Animal Health; Kansas City, MO).

Animal surgery. Twenty-one adult male rats were used in this study. Three rats underwent a sham operation with a 1-cm skin incision made along the inferior border of the right mandible, separation of the rat masseter muscle, and exposure of the mandible without performing an osteotomy. In 18 experimental animals, the body of the right hemimandible was similarly exposed; however an osteotomy was performed in a copiously irrigated field between the second and third molars (Fig. 1) with an 8-mm, double-sided diamond disc (Brassler, Savannah, GA). A pair of 1-mm bicortical holes were drilled 4 mm anterior and posterior to the osteotomy and two 1.5 × 20-mm Flexi-Post pins (Essential Dental Systems, South Hackensack, NJ) were screwed into the holes. A prefabricated external fixator was attached to the pins (Fig. 1). The field was irrigated copiously with sterile saline, and the skin and soft tissues were reapproximated with resorbable sutures. Buprenorphine (0.1 mg/kg; Fort Dodge Animal Health) was administered for 1 day postoperatively for pain management. Twelve animals were killed on postoperative *days 3*, *9*, and *23*; the right hemimandible was dissected free of skin and soft tissues; and the section of the mandible immediately bounded by the pins was resected, snap frozen in liquid nitrogen, and homogenized with a Polytron tissue homogenizer (Kinematica). Total cellular RNA was extracted with TRIzol solution as outlined below. In the remaining six animals, mandibles harvested on postoperative *days 9* and *23* were fixed in 4% paraformaldehyde and decalcified in Immunocal (Decal Chemical, Congers, NY) for 6 days. Tissues were then placed in 30% sucrose solution for 2 days and embedded in tissue-freezing medium (Triangle Biomedical Sciences, Durham, NC), and 10-mm sections were prepared for immunohistochemistry as outlined below.

Probe preparation. Glyceraldehyde-3-phosphate dehydrogenase (GAPDH) was a 1-kb probe from Clontech (Palo Alto,

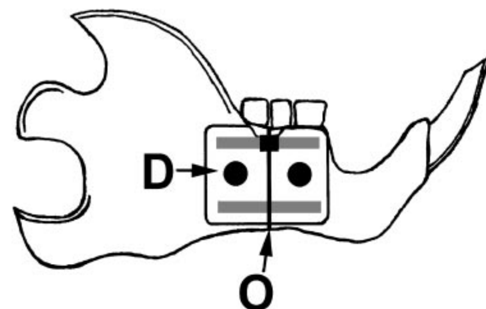

Fig. 1. Schematic of rat mandible demonstrating osteotomy (O) and external fixator (D). An osteotomy was performed in a copiously irrigated field between the 2nd and 3rd molars. A pair of 1-mm bicortical holes were drilled 4 mm anterior and posterior to the osteotomy, 2 1.5 × 20-mm pins were screwed into the holes, and a prefabricated external fixator was attached to the pins.

CA). A 535-bp probe against rat TGF-β1 and a 411-bp probe against mouse VEGF were generated by PCR from whole rat and mouse embryo cDNA, respectively (16). PCR primers for TGF-β1 and VEGF have been previously described (4, 15). PCR bands were gel purified, cloned into PCR.1 plasmids (Invitrogen, Carlsbad, CA), and sequenced to confirm sequence identity. The probe was generated after *Eco*R I digestion and gel purification. One hundred nanograms of each probe were labeled with ^{32}P-labeled deoxycytidine triphosphate ([α-^{32}P]dCTP) by using random oligonucleotide primers and Klenow fragment (Ready To Go labeling beads; Pharmacia Biotech, Cambridge, England). Unincorporated nucleotides were removed with Sephadex G-50 DNA-grade nick columns (Pharmacia Biotech). All probes had specific activities $>10^5$ cpm/ml of hybridization solution.

RNA extraction and Northern analysis. Subconfluent FRC (*passage 2*) and MC3T3-E1 cells in 100-mm^2 plates were stimulated with 2.5 ng/ml TGF-β1 in antibiotic-containing, serum-free media for 0, 3, 6, or 24 h. In experiments designed to investigate the effect of TGF-β1 on VEGF mRNA stability, transcription was interrupted with actinomycin D (5 µg/ml) after 2 h of stimulation with TGF-β1 (2.5 ng/ml) in serum-free media. To investigate protein synthesis or gene transcription, subconfluent MC3T3-E1 cells in 100-mm^2 plates underwent 3-h exposures to cycloheximide (10 µg/ml) or actinomycin D (5 µg/ml) with or without TGF-β1 (2.5 ng/ml; ±TGF-β1). Cells in the actinomycin D group (but not the cycloheximide group) underwent 1 h of pretreatment with actinomycin D before TGF-β1 stimulation (14).

Experiments were designed to disrupt TGF-β1 signal transduction. The dominant-negative truncated TGF-β receptor II adenovirus and a β-galactosidase adenovirus have been previously described and characterized in endothelial cells (39) and in MC3T3-E1 clonal osteoblasts (Mehrara and Saadeh, unpublished results). At a multiplicity of infection (MOI) of 100, cells are efficiently transfected and strongly overexpress the dominant-negative truncated TGF-β receptor II. After binding TGF-β (all isoforms), this receptor is unable to phosphorylate TGF-β receptor I, thus interrupting intracellular signaling. An adenovirus containing the β-galactosidase gene served as a viral infection control. Subconfluent MC3T3-E1 cells in T75 flasks were infected with vehicle (PBS with 10% glycerol), the dominant-negative truncated TGF-β receptor II adenovirus, or the β-galactosidase adenoviral control (MOI = 100). After 60 h of incubation, cells were stimulated with 2.5 ng/ml TGF-β1 in antibiotic-containing, serum-free media for 0, 3, 6, or 24 h, after which total cellular RNA was harvested and VEGF mRNA levels were analyzed by Northern blotting.

Northern blot analysis. Total cellular RNA was extracted with TRIzol solution (Life Technologies) according to the manufacturer's specifications, and quantified with an Ultraspec2000 spectrophotometer (Pharmacia Biotech). RNA integrity was assessed by ethidium bromide staining of 18S and 28S ribosomal bands. Twenty micrograms of total cellular RNA were loaded onto a 1.0% denaturing formaldehyde gel and resolved by electrophoresis. RNA was transferred to positively charged 0.45-µm nylon membranes (Schleicher & Schuell, Keene, NH), and UV cross-linked for 2 min (Stratagene, La Jolla, CA) to link the RNA to the membranes. Membranes were prehybridized for 1–2 h at 68°C in ExpressHyb hybridization solution (Clontech); this was followed by hybridization with [α-^{32}P]dCTP-labeled cDNA probes against VEGF, TGF-β1, or GAPDH in fresh Rapid Hybridization solution (Clontech) for 2 h at 68°C. Stringency washes were performed twice at room temperature with 2× SSC (1× SSC = 0.15 M NaCl-15 mM sodium citrate)-0.1% SDS for 10 min each and were followed by two washes in 0.1× SSC-0.1% SDS at 50°C for 15 min each. Membrane signal intensity was quantified with a PhosphorImager (Molecular Dynamics, Sunnyvale, CA), and the resulting images were analyzed with ImageQuant (Molecular Dynamics) image analysis software. All experiments were repeated in triplicate.

VEGF concentration in conditioned media. A mouse VEGF quantitative sandwich enzyme immunoassay was purchased from R&D Systems (Minneapolis, MN). Assay and controls were performed in accordance with the manufacturer's recommendations. Briefly, 2×10^4 MC3T3-E1 cells were plated in each well of a 24-well plate and allowed to reach confluence over a period of 2–3 days in DMEM supplemented with 10% FBS as described above. Once at confluence, media were removed and cells were washed with PBS. Serum free media (400 µl) containing an antibiotic and antimycotic and recombinant human TGF-β1 in concentrations of 0, 0.62, 1.25, 2.5, 5, 12.5, and 25 ng/ml were then added to the cultures. Additionally, as a separate experiment, dexamethasone (1×10^{-7}, 2×10^{-7}, and 4×10^{-7} M) was coadded to separate wells stimulated with 5 ng/ml TGF-β1. Each cytokine dose was repeated four times per experiment. After 24 h, the media were removed and centrifuged to remove particulate matter. Equal cell numbers between wells were further verified by a crystal violet colorimetric assay (see below). All experiments were repeated in triplicate.

Crystal violet staining. To minimize the effect of alterations in cellular proliferation or equal plating, the number of plated cells was estimated by crystal violet staining as described by Kueng et al. (22). Briefly, cells were washed in PBS and fixed in ice-cold 3.7% paraformaldehyde (Sigma) for 20 min. Cells were washed with PBS, permeablized with 20% methanol for 20 min, and stained with 0.5% crystal violet (Sigma) in 20% methanol for 30 min. Excess stain was removed after washes in deionized water, followed by elution with 10% acetic acid for 30 min. The optical density of the dye was measured at 650 nm with a SPECTRAmax 250 spectrophotometer (Molecular Devices, Sunnyvale, CA).

Immunohistochemistry. Affinity-purified rabbit polyclonal anti-TGF-β1 and anti-VEGF antibodies with no cross-reactivity were used in all experiments (R&D Systems). After fixing fracture tissues from *days 9* and *23*, immunohistochemistry was performed as previously described (32). Briefly, 10-µm tissue sections were placed on SuperFrost Plus slides (Fisher Scientific), endogenous peroxidase activity was quenched with 0.6% hydrogen peroxide in methanol, and antigen unmasking was performed with 10 mM sodium citrate. Nonspecific staining was blocked by incubating sections with normal goat serum (1.5%; Vector Laboratories, Burlingame, CA) followed by antisera against TGF-β1 or VEGF overnight at 4°C. Biotinylated goat anti-rabbit secondary antibodies (Vector Laboratories) and avidin-biotin peroxidase complex were successively applied, and positive staining was visualized with 3,3′diaminobenzidine (Sigma) as the substrate to cause brown staining of positively stained tissues. Sections were counterstained with Harris hematoxylin. Control slides were incubated in nonimmune rabbit serum or no primary antibody and processed identically to experimental sections. All experiments were performed in triplicate.

Statistical analysis. All data from the quantitative VEGF sandwich enzyme immunoassay are expressed as means ± SD. Additionally, the quantitative sandwich enzyme immunoassay and the crystal violet assay underwent statistical significance testing with one-way ANOVA to compare levels of VEGF protein production by the different doses of TGF-β1. Post hoc tests consisted of the Tukey-Kramer multiple comparison test, with $P < 0.05$ considered significant.

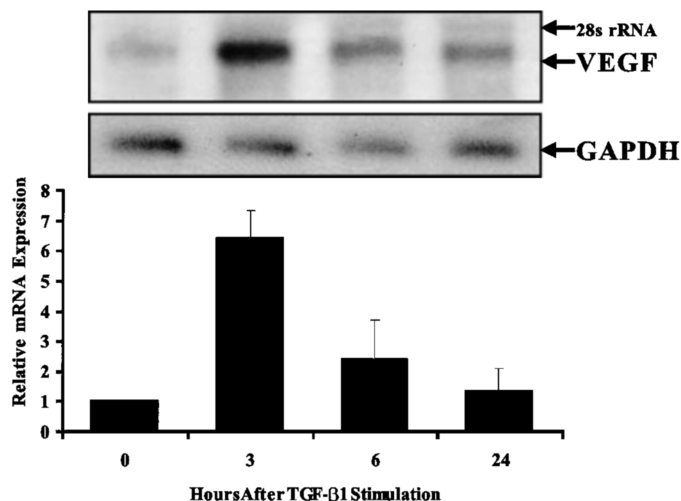

Fig. 2. Transforming growth factor-β1 (TGF-β1) increased vascular endothelial growth factor (VEGF) mRNA levels in MC3T3-E1 osteoblast-like cells. MC3T3-E1 cells were treated with TGF-β1 (2.5 ng/ml) for indicated times, from 0 to 24 h. Total cellular RNA (20 µg/lane) was subjected to blot analysis with a mouse VEGF cDNA probe, and resulting signal intensity was quantified with a PhosphorImager (*top bands*). *Bottom bands*, glyceraldehyde-3-phosphate dehydrogenase (GAPDH) probe hybridized to same filter, after stripping, provides a comparison of RNA loading. Figure represents results from 1 of 3 similar experiments. Graph shows quantification of relative VEGF mRNA at indicated time points. Intensity of VEGF hybridization is given as a value relative to that for unstimulated MC3T3-E1 cells. Data are means of 3 experiments ± SD. VEGF mRNA was increased 6-fold at 3 h with lower, but still elevated, levels at 6 and 24 h.

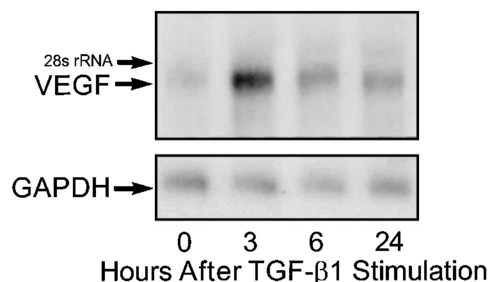

Fig. 3. Effect of TGF-β1 on VEGF mRNA in fetal rat calvarial (FRC) cells. FRC cells were treated with TGF-β1 (2.5 ng/ml) for indicated times, from 0 to 24 h. Total cellular RNA (20 µg/lane) was subjected to blot analysis with a mouse VEGF cDNA probe (*top bands*). *Bottom bands*, GAPDH probe hybridized to same filter, providing a comparison of RNA loading. VEGF mRNA was increased at 3 h with lower, but still elevated, levels at 6 and 24 h. Figure represents results from 1 of 2 similar experiments.

RESULTS

TGF-β1 increased VEGF mRNA levels in MC3T3-E1 osteoblast-like cells and primary osteoblasts. MC3T3-E1 mouse clonal osteoblasts express osteoblastic features such as collagen type I and alkaline phosphatase and they behave similarly to primary osteoblasts in response to TGF-β1 (3). When osteoblastic cells were stimulated with 2.5 ng/ml TGF-β1, VEGF mRNA was increased at all time points compared with levels in unstimulated cells (Fig. 2). Maximal VEGF mRNA occurred early, with a 6-fold increase in VEGF mRNA at 3 h followed by decreases to 2.5- and 1.5-fold inductions of VEGF mRNA expression at 6 and 24 h respectively. Similarly, when the FRC cells were stimulated with 2.5 ng/ml TGF-β1, VEGF mRNA was increased at all time points compared with levels in unstimulated cells and the peak increase occurred at 3 h (Fig. 3). Importantly, the concentration of TGF-β1 added to the cell cultures falls within the range of previously reported physiologically relevant levels (~1 ng/ml).

Effect of mRNA and protein synthesis inhibitors on TGF-β1 stimulation of VEGF mRNA. The short, sharp rise of VEGF mRNA followed by its rapid decline in TGF-β1-stimulated primary osteoblasts and osteoblastic cells was consistent with the pattern shown by other osteogenic cytokines (19) and suggested high turnover and low stability of VEGF mRNA. To further define the mechanisms of action of TGF-β1 stimulation of VEGF expression in osteoblastic cells, we employed inhibitors of RNA polymerase and protein synthesis to block transcription and translation, respectively (Fig. 4). Blockade of transcription with actinomycin D (5 µg/ml) decreased the baseline VEGF mRNA. When protein production was blocked with cycloheximide (10 µg/ml), VEGF mRNA was still produced. The TGF-β1-induced increase in VEGF expression was blocked by actinomycin D. In contrast, disruption of translation with cycloheximide did not substantially reduce VEGF mRNA expression in response to TGF-β1 stimulation, suggesting that TGF-β1 exerted its effects at the transcriptional level.

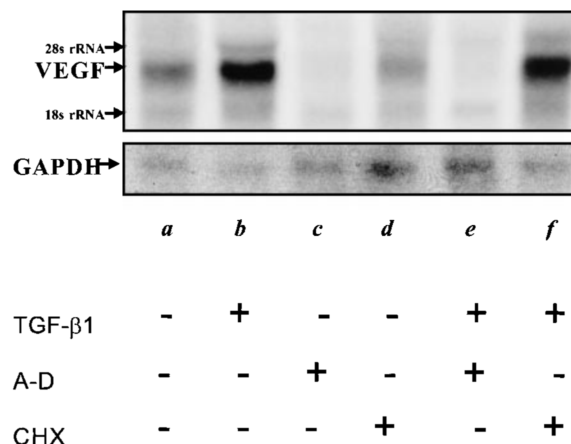

Fig. 4. Effect of RNA and protein synthesis inhibitors on TGF-β1 stimulation of VEGF mRNA. MC3T3-E1 cells underwent 3-h exposures to 5 µg/ml actinomycin D (*A-D*) or 10 µg/ml cycloheximide (CHX), with (+) or without (−) TGF-β1 (2.5 ng/ml). Cells in the actinomycin D group underwent 1 h of pretreatment with actinomycin D before TGF-β1 stimulation. Total cellular RNA (20 µg/lane) was subjected to blot analysis with a mouse VEGF cDNA probe. *Bottom band*, GAPDH probe hybridized to same filter, after stripping, provides a comparison of RNA loading. Blockade of transcription with actinomycin resulted in decrease of the baseline VEGF mRNA (*lane c*). When protein production was blocked with cycloheximide (10 µg/ml), VEGF mRNA was still produced (*lane d*). Pretreatment with actinomycin D blocked the TGF-β-induced increase in VEGF expression (*lane e*). In contrast, disruption of translation with cycloheximide did not significantly reduce VEGF mRNA expression in response to TGF-β1 stimulation (*lane f*). Figure represents results from 1 of 2 similar experiments.

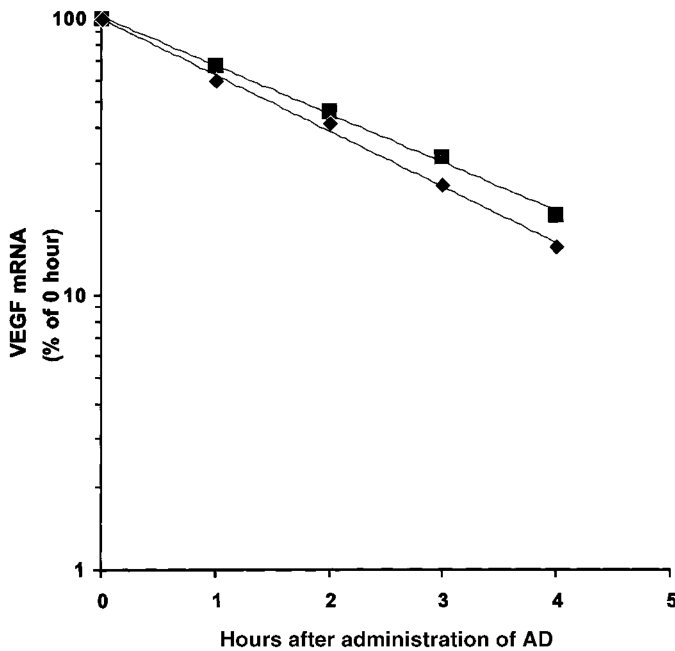

Fig. 5. Effect of TGF-β1 stimulation of MC3T3-E1 osteoblast-like cells on VEGF mRNA stability. Two hours after treatment with either vehicle (◆) or 2.5 ng/ml TGF-β1 (■), transcription was inhibited by actinomycin D (AD; 5 µg/ml). Total cellular RNA was isolated at indicated time points, and 20 µg RNA/lane were resolved on a denaturing gel; this was followed by transfer to a nylon membrane. RNA was then subjected to blot analysis with a labeled mouse VEGF cDNA, and resulting signal intensity was quantified with a PhosphorImager. Membranes were then stripped and rehybridized to a labeled GAPDH probe. Small differences in loading were accounted for by dividing signal for VEGF intensity by respective GAPDH signal intensity. Relative amount of VEGF mRNA was expressed as a percentage of 0-h values. Data represent results of 1 of 2 similar experiments.

To further elucidate the mechanisms of action of TGF-β1 stimulation on VEGF mRNA expression, we compared the stability of VEGF mRNA produced by unstimulated osteoblastic cells to the stability of VEGF mRNA produced by cells stimulated with TGF-β1 (Fig. 5). Two hours after treatment with either vehicle or TGF-β1, transcription was inhibited by the addition of actinomycin D. The VEGF mRNA half-life of cells treated with TGF-β1 was not significantly different from the half-life of vehicle-treated cellular mRNA, indicating that the rapid upregulation of VEGF mRNA by TGF-β1 is largely transcriptionally (and not mRNA stabilization) mediated.

TGF-β signal blockade reduced TGF-β1 stimulation of VEGF mRNA. TGF-β has three defined isoforms in mammals, TGF-β1, TGF-β2, and TGF-β3. In addition to effecting differential modulation of gene expression, these isoforms may act through autocrine mechanisms to regulate both their own expression and the expression of their common receptor, transforming growth factor receptor II. Although neutralizing antibody studies are an effective way to isolate cytokine effects, the multiple isoforms of TGF-β, and the biphasic effects of TGF-β1 in particular, make TGF receptor II an elegant target for manipulation. Overexpression of a dominant-negative TGF receptor II via an adenovirus vector allowed for disruption of TGF-β signal transduction because this construct binds all TGF-β isoforms but does not allow phosphorylation of TGF-β receptor I. When exogenous TGF-β1 was added to control (uninfected or β-galactosidase adenovirus-infected) cells, the previously described increase in VEGF expression (peak at 3 h) was identified (Fig. 6). However, when cells were transfected with truncated dominant-negative TGF receptor II, the expression of VEGF was significantly curtailed at all time points. These data are further evidence that TGF-β1 acts through its secondary receptors to directly effect the upregulation of VEGF mRNA.

Effect of TGF-β1 on VEGF concentration in conditioned medium. We then proceeded to examine the production of VEGF protein as a result of TGF-β1 stimulation. Additionally, we examined the dose-response relationship between TGF-β1 and VEGF. The basal level of VEGF production by MC3T3-E1 cells was 300 pg/ml at 24 h (Fig. 7). To control for the effect that TGF-β1 may have had on cell proliferation, only identically seeded, confluent wells were stimulated with TGF-β1. Additionally, a crystal violet assay, performed at the time of medium collection, did not demonstrate statistically significant well-to-well variation in cell number (data not shown). TGF-β1 produced a dose-dependent increase in VEGF production with a maximal increase to 1,200 pg/ml at 25 ng/ml TGF-β1. At 2.5 ng/ml TGF-β1, VEGF production was 1,050 pg/ml. Thereafter, the slope of VEGF production decreased to a plateau, suggesting receptor saturation. TGF-β1 had a significant effect on VEGF protein production at the physiologically relevant doses of 0.63 and 1.25 ng/ml, with increases in VEGF production to 600 and 900 pg/ml, respectively.

Effect of dexamethasone on TGF-β1-stimulated VEGF production in conditioned medium. To consider the effects of glucocorticoids on TGF-β1-induced VEGF expression in bone, dexamethasone was added to the culture system. Dexamethasone significantly inhibited TGF-β1 stimulation of VEGF expression in a dose-dependent fashion (Fig. 8). This decrease in a potential angiogenic response may provide an insight into the molecular mechanisms of glucocorticoid impairment of bone healing.

TGF-β1 and VEGF mRNA are coexpressed during membranous bone fracture healing in vivo. Having identified the effect of TGF-β1 on VEGF expression by osteoblasts in vitro, we investigated the presence of TGF-β1 and VEGF in vivo in both unfractured and fractured membranous bone. An osteotomy was created behind the second molar of the rat right hemimandible, and a mandibular fixation device was applied as shown in Fig. 1. Total cellular RNA was isolated from fractured rat mandibles (3, 9, and 23 days after the operation) and was analyzed by Northern blotting with a TGF-β1 probe. TGF-β1 mRNA was identified at all time points and increased with time after fracture (Fig. 9). The greatest TGF-β1 mRNA signal occurred at 23 days, the middle period of fracture consolidation. We next sought to identify the concurrent presence of VEGF mRNA. Therefore, identical specimens of total

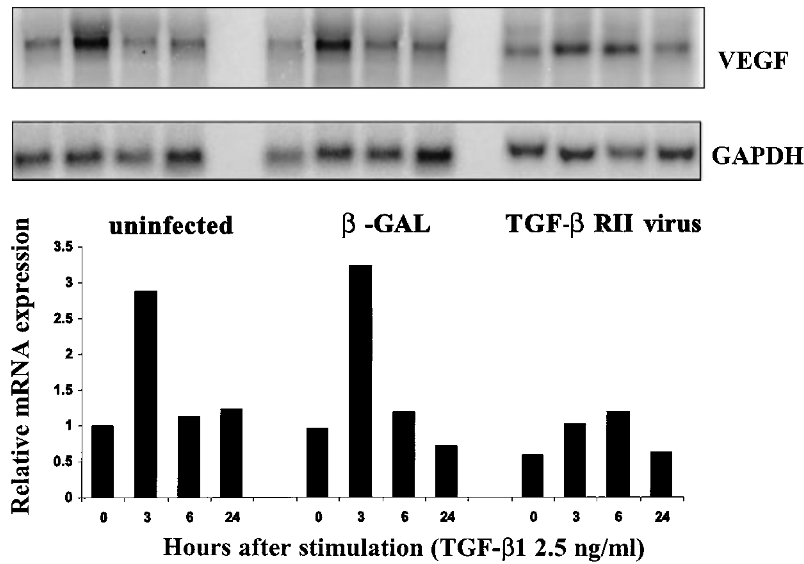

Fig. 6. Effect of TGF-β signal blockade on TGF-β1 stimulation of VEGF mRNA. MC3T3-E1 osteoblastic cells were infected with the β-galactosidase adenoviral control (β-GAL) or the dominant-negative truncated TGF-β receptor II adenovirus (multiplicity of infection = 100). After 60 h of incubation, cells were stimulated with 2.5 ng/ml TGF-β1 in antibiotic-containing, serum-free media for 0, 3, 6, or 24 h. Total cellular RNA was isolated and 20 μg RNA/lane were resolved on a denaturing gel; this was followed by transfer to a nylon membrane. RNA was then subjected to blot analysis with a labeled mouse VEGF cDNA, and resulting signal intensity was then quantified with a PhosphorImager. Membranes were then stripped and rehybridized to a labeled GAPDH probe. Uninfected control cells demonstrated a pattern of VEGF mRNA expression similar to that identified in earlier experiments, with a peak increase at 3 h and lower (but above baseline) levels at 6 and 24 h. β-Galactosidase adenovirus-infected cells demonstrated an identical pattern of VEGF mRNA expression with, again, a peak increase at 3 h and lower (but above baseline) levels at 6 and 24 h. Adenoviral infection, by itself, did not alter the response of the cells to TGF-β1. Competitive binding of TGF-β1 to an overexpressed truncated TGF-β receptor II adenovirus substantially interfered with TGF-β1 signal transduction, resulting in a very blunted response to TGF-β1 stimulation noted particularly at 3 h, the normal peak of stimulated VEGF mRNA expression.

cellular RNA from fractured rat mandibles were analyzed by Northern blotting with a mouse VEGF probe (Fig. 9). As found for TGF-β1, VEGF mRNA increased during fracture healing with the strongest increase also occurring 23 days after fracture. Interestingly, at 9 days after the operation, the increase in VEGF mRNA appeared greater than the increase in TGF-β1 mRNA. Finally, unfractured mandibles revealed levels of TGF-β1 and VEGF mRNA similar to those at 23 days after the operation (data not show).

TGF-β1 and VEGF proteins are both present in the fracture callus during membranous fracture healing. Immunohistochemical staining of a fracture site revealed the presence of both TGF-β1 and VEGF (Figs. 10

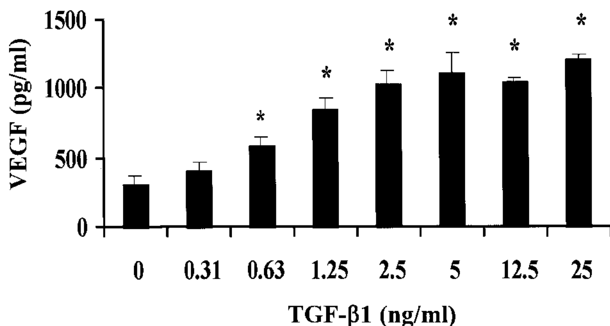

Fig. 7. Effect of TGF-β1 on VEGF protein production in culture media of MC3T3-E1 cells. MC3T3-E1 cells were cultured for 24 h in serum-free media containing indicated doses of TGF-β1. Media were collected, and VEGF was quantified with a mouse VEGF quantitative sandwich enzyme immunoassay. Data are means of 3 experiments ± SD. TGF-β1 produced a dose-dependent increase in VEGF production, with a plateau of VEGF beginning at 2.5 ng/ml TGF-β1. At doses of TGF-β1 > 0.31 ng/ml, levels of VEGF protein production were significantly greater than those for unstimulated group (* $P < 0.01$).

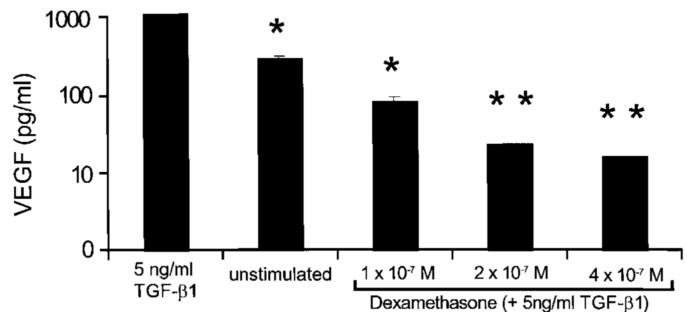

Fig. 8. Effect of dexamethasone on VEGF protein production by TGF-β1-treated MC3T3-E1 cells. MC3T3-E1 cells were cultured for 24 h in serum-free media containing 5 ng/ml TGF-β1 and indicated doses of dexamethasone. Media were collected, and VEGF was quantified with a mouse VEGF quantitative sandwich enzyme immunoassay. The *y*-axis is represented logarithmically. Data are means of 3 experiments ± SD (lack of error bars indicates small SD that cannot be represented on this logarithmic graph). There were statistically significant differences between all the groups (* $P < 0.01$). ** Groups not statistically different from each other but statistically different from all remaining groups ($P < 0.01$). Dexamethasone produced a dose-dependent decrease in VEGF production.

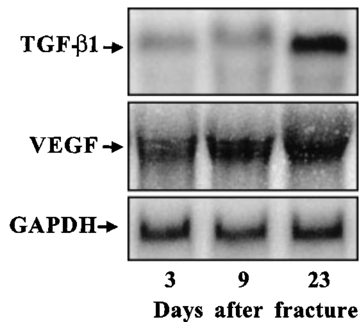

Fig. 9. *Top 2 bands*, TGF-β1 mRNA and VEGF mRNA in rat mandibular fracture site during healing. An osteotomy was created in right mandible of each rat, and a fixation device was applied. Total cellular RNA was isolated from fracture tissues at 3, 9, and 23 days, and RNA (30 μg/lane) was subjected to blot analysis with a rat TGF-β1 cDNA probe or a mouse VEGF cDNA probe. Arrows, locations of TGF-β1 and VEGF mRNA. *Bottom band*, GAPDH band providing a comparison of RNA loading. Northern blots represent 1 of 3 similar experiments.

and 11). As the bone healed, TGF-β1 was strongly localized to the fracture callus and the proliferating osteoblasts within and immediately surrounding the callus (Fig. 10, *A-D*). Likewise, throughout fracture healing, the fracture callus demonstrated strong VEGF staining, as did the proliferating osteoblasts within and immediately surrounding the callus (Fig. 11, *A-F*). TGF-β1 staining was both cytoplasmic and matrix associated, whereas VEGF staining was primarily cytoplasmic. Furthermore, although osteoblasts stained strongly for VEGF, osteocytes did not appear to be expressing VEGF, suggesting tightly localized control of VEGF expression. Control groups (nonimmune rabbit serum or no primary antibody) did not demonstrate positive staining (data not shown).

DISCUSSION

The wide-ranging presence and effects of TGF-β1 underscore its fundamental role as an orchestrator of biomolecular events. Furthermore, its ubiquitous nature and sometimes discrepant effects both encourage and complicate its study. It has been observed that TGF-β1 can stimulate or inhibit angiogenesis in vivo. For example, TGF-β1 promotes angiogenesis in both the rabbit corneal micropocket (30) and the chick chorioallantoic membrane (40) models. In contrast, genetically induced TGF-β1 overexpression in arteries, liver, epidermis, and respiratory epithelial cells does not result in angiogenesis (28). Additionally, TGF-β1 inhibits both cultured endothelial cell proliferation (1) and fibroblast growth factor (FGF)-induced angiogenesis in a subcutaneous sponge system (27). These apparently discrepant effects have given rise to the notion that the microenvironment within which TGF-β1 is expressed determines TGF-β1's ultimate biological effects. More specifically, it has been observed that, within the context of inflammation, increased TGF-β1 levels correlate with increased angiogenesis (28). This biology may be due, in part, to the presence of a specialized, recruited subset of inflammatory cells, which are known to produce both inflammatory and angiogenic cytokines. This, in turn, is consistent with the concept that TGF-β1 is an indirect cytokine of angiogenesis. Thus, given the proper environment and/or effector cells, TGF-β1 can be involved in the production of direct angiogenic factors such as VEGF.

Because the fracture milieu contains many of the conditions and factors that have, in other tissues, been found to promote VEGF expression [hypoxia (20, 35), elevated TGF-β1 (5), FGF-2 (26), and interleukin-1 (20)], we sought to isolate the effect of TGF-β1 on VEGF

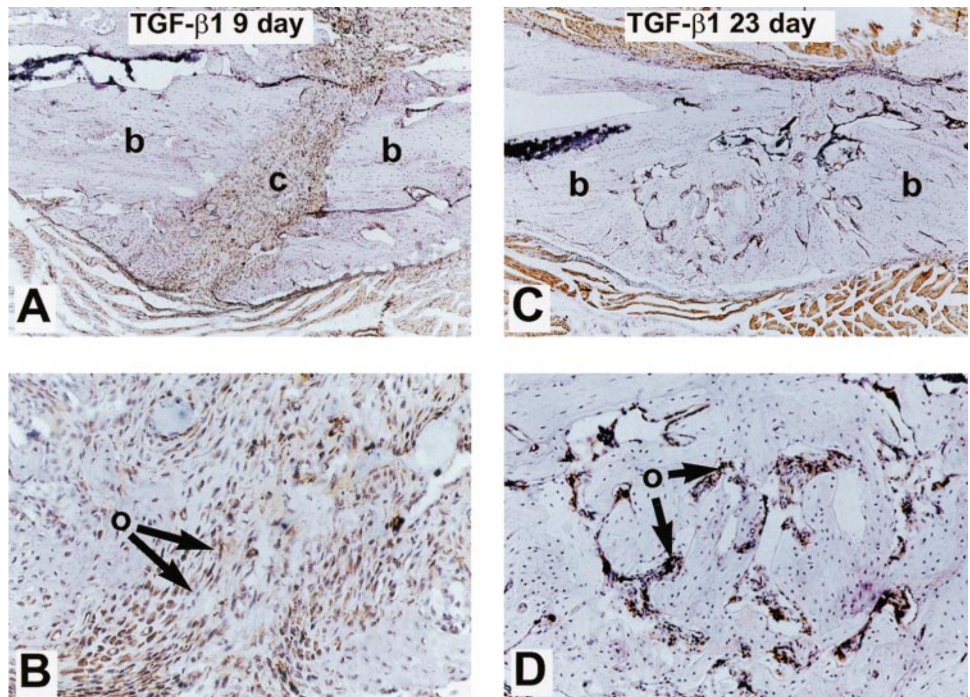

Fig. 10. Localization of TGF-β1 protein during rat mandibular fracture healing. An osteotomy was created in right mandible of each rat, and a fixation device was applied. After fixing fracture tissue from mandibles harvested 9 and 23 days after operation, immunohistochemistry was performed with affinity-purified rabbit polyclonal anti-TGF-β1. Sections were counterstained with Harris hematoxylin. *A* and *B*: low- (×10) and medium (×20)-power views of fracture site 9 days after osteotomy. *C* and *D*: low- (×10) and medium (×20)-power views of fracture site 23 days after osteotomy. b, Bone; c, callus; o, osteoblasts.

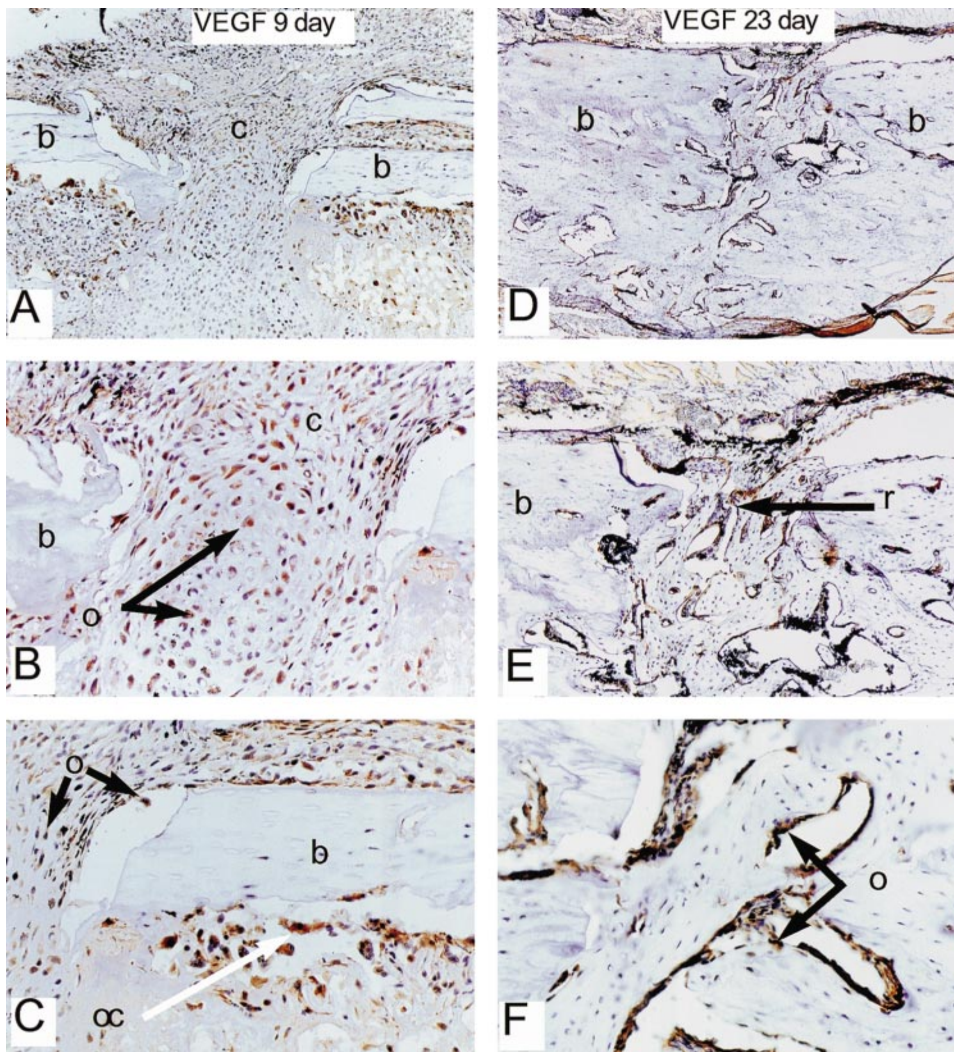

Fig. 11. Localization of VEGF protein during rat mandibular fracture healing. An osteotomy was created in right mandible of each rat, and a fixation device was applied. After fixing fracture tissue from mandibles harvested 9 and 23 days postoperatively, immunohistochemistry was performed with affinity-purified rabbit polyclonal anti-VEGF. Sections were counterstained with Harris hematoxylin. *A-C*: low- (×10), medium- (×20), and high (×50)-power views of fracture site 9 days after osteotomy. *D-F*: low- (×10), medium- (×20), and high (×50)-power views of fracture site 23 days after osteotomy. b, Bone; c, callus; o, osteoblasts; oc, osteoclasts; r, remodeling bone.

production by osteoblastic cells in vitro. We found that TGF-β1 increased the expression of VEGF mRNA by primary osteoblasts and osteoblastic cells. This effect occurred at a dose of 2.5 ng/ml TGF-β1, which lies within the mammalian physiological range and is similar to the concentration that upregulates VEGF mRNA in vascular smooth muscle cells (5).

The TGF-β1-induced increase in VEGF mRNA appears to be primarily a transcriptionally mediated event. As found for IGF-I, PGE_1, and PGE_2, VEGF mRNA stability was unaffected by TGF-β1, whereas actinomycin D, but not cycloheximide, strongly decreased TGF-β1 induction of VEGF mRNA. When TGF-β1 signal transmission was disrupted by an overexpressed dominant-negative receptor II, the increase in VEGF mRNA was greatly attenuated.

Although the peak increase in VEGF mRNA was acute, VEGF mRNA remained elevated throughout the stimulation period. Furthermore, TGF-β1 stimulated a dose-dependent increase in VEGF protein production by MC3T3-E1 osteoblastic cells, and this response began at physiologically relevant TGF-β1 doses. These observations were consistent with our in vivo findings of VEGF mRNA expression during fracture healing and localization of VEGF protein to a healing fracture callus. The mitogenic and remodeling effect of VEGF on capillary endothelial cells and the ability of TGF-β1 to increase VEGF expression by the endothelium suggest that TGF-β1 plays an important role in the angiogenic response evidenced by healing bone.

The impairment of the vascular supply to bone results in avascular necrosis (6). Traditional theories regarding the mechanism of glucocorticoid-induced avascular necrosis center on abnormal fat metabolism, with resultant fat embolism causing vascular occlusion and subsequent bone death (7). Smith (36) has hypothesized that the pathogenesis of avascular necrosis of the femoral head is based on the inhibition of angiogenesis. Dexamethasone has been shown to inhibit angiogenesis in vitro (18) and to block prostaglandin stimulation of VEGF production in osteoblastic cells (19). In vitro, dexamethasone produced a dose-dependent inhibition of TGF-β1-induced VEGF protein production and may provide an additional molecular explanation for the well-observed phenomenon of both impaired fracture vascularization and healing in glucocorticoid-treated patients.

We also demonstrated the concurrent presence of TGF-β1 and VEGF mRNA in bone. Additionally, we found that, during membranous bone fracture healing, TGF-β1 and VEGF mRNAs have similar patterns of expression, with both being expressed during early fracture healing and both increasing during mineralization. Although the increase in VEGF mRNA at 9 days after the operation was greater than that of TGF-β1 mRNA, this may simply be testimony to the potency of TGF-β1 as an inducer of VEGF production. Additionally, the increase of VEGF during this inflammatory phase may be, at least partially, an indirect effect of TGF-β1, because TGF-β1 increases the levels of several cytokines (FGF-2, and TGF-β1 itself) that have been implicated in VEGF expression. Finally, the effect of TGF-β1 on VEGF may by synergistically enhanced by other cytokines and conditions (strain, hypoxia) present in the fracture milieu. Immunohistochemical analysis of the fracture site was consistent with the mRNA findings and revealed strong staining of osteoblasts within the fracture callus for both TGF-β1 and VEGF protein. Administration of exogenous recombinant TGF-β1 protein has been shown to promote healing of both endochondral fractures (24) and membranous defects (2). A fracture creates the necessary environment for release of TGF-β1 from platelets and bone (the largest two reservoirs of latent TGF-β1), activation of latent TGF-β1 by acidic conditions and plasminogen (41), and upregulation of TGF-β1 expression in an autocrine and paracrine fashion (31). It is likely that this inflammatory microenvironment sets the stage for the production of VEGF and other direct angiogenic cytokines, without which fracture vascularization and, hence, healing cannot occur.

These data further advance the concepts of contextual and indirect activity of TGF-β1 as a promoter of angiogenesis. Both the in vivo and the in vitro findings supplement the current understanding of the fracture microenvironment. It is likely that VEGF is produced and acts in concert with a multitude of other factors involved in angiogenesis during fracture healing. We are actively defining these factors and their interrelationships. We remain hopeful that further understanding of angiogenic mechanisms in bone healing will provide the foundation for therapeutic molecular manipulations to improve bone healing.

Address for reprint requests and other correspondence: M. T. Longaker, Laboratory of Developmental Biology and Repair, Rm. H-169, New York Univ. Medical Center, 550 First Ave., New York, NY 10016 (E-mail: michael.longaker@med.nyu.edu).

Received 5 February 1999; accepted in final form 2 June 1999.

REFERENCES

1. **Baird, A., and T. Durkin.** Inhibition of endothelial cell proliferation by type beta-transforming growth factor: interactions with acidic and basic fibroblast growth factors. *Biochem. Biophys. Res. Commun.* 138: 476–482, 1986.
2. **Beck, L. S., E. P. Amento, Y. Xu, L. Deguzman, W. P. Lee, T. Nguyen, and N. A. Gillett.** TGF-beta 1 induces bone closure of skull defects: temporal dynamics of bone formation in defects exposed to rhTGF-beta 1. *J. Bone Miner. Res.* 8: 753–761, 1993.
3. **Bonewald, L. F., and G. R. Mundy.** Role of transforming growth factor beta in bone remodeling: a review. *Connect. Tissue Res.* 23: 201–208, 1989.
4. **Breitbart, A. S., D. A. Staffenberg, C. H. Thorne, P. M. Glat, N. S. Cunningham, A. H. Reddi, J. Ricci, and G. Steiner.** Tricalcium phosphate and osteogenin: a bioactive onlay bone graft substitute. *Plast. Reconstr. Surg.* 96: 699–708, 1995.
5. **Brogi, E., T. Wu, A. Namiki, and J. Isner.** Indirect angiogenic cytokines upregulate VEGF and bFGF gene expression in vascular smooth muscle cells, whereas hypoxia upregulates VEGF expression only. *Circulation* 90: 649–652, 1994.
6. **Burkhardt, R., G. Kettner, W. Bohm, M. Schmidmeier, R. Schlag, B. Frisch, B. Mallmann, W. Eisenmenger, and T. Gilg.** Changes in trabecular bone, hematopoiesis and bone marrow vessels in aplastic anemia, primary osteoporosis, and old age: a comparative histomorphometric study. *Bone* 8: 157–164, 1987.
7. **Chang, C. C., A. Greenspan, and M. E. Gershwin.** Osteonecrosis: current perspectives on pathogenesis and treatment. *Semin. Arthritis Rheum.* 23: 47–69, 1993.
8. **Collin-Osdoby, P.** Role of vascular endothelial cells in bone biology. *J. Cell. Biochem.* 55: 304–309, 1994.
9. **Cruess, R. L.** Osteonecrosis of bone. Current concepts as to etiology and pathogenesis. *Clin Orthop*: 30–39, 1986.
10. **Cutting, C., and J. McCarthy.** Comparison of residual osseous mass between vascularized and nonvascularized onlay bone transfers. *Plast. Reconstr. Surg.* 72: 672–675, 1983.
11. **Dodds, R. A., K. Merry, A. Littlewood, and M. Gowen.** Expression of mRNA for IL1-β, IL6, and TGF-β1 in developing human bone and cartilage. *J. Histochem. Cytochem.* 42: 733–744, 1994.
12. **Ferrara, N., K. Carver-Moore, H. Chen, M. Dowd, L. Lu, K. S. O'Shea, L. Powell-Braxton, K. J. Hillan, and M. W. Moore.** Heterozygous embryonic lethality induced by targeted inactivation of the VEGF gene. *Nature* 380: 439–442, 1996.
13. **Freshney, R. I.** *Culture of Animal Cells: a Manual of Basic Technique*. New York: Liss, 1994, p. 332–333.
14. **Goad, D. L., J. Rubin, H. Wang, A. H. Tashjian, Jr., and C. Patterson.** Enhanced expression of vascular endothelial growth factor in human SaOS-2 osteoblast-like cells and murine osteoblasts induced by insulin-like growth factor I. *Endocrinology* 137: 2262–2268, 1996.
15. **Goede, V., T. Schmidt, S. Kimmina, D. Kozian, and H. G. Augustin.** Analysis of blood vessel maturation processes during cyclic ovarian angiogenesis. *Lab. Invest.* 78: 1385–1394, 1998.
16. **Gombotz, W., and D. Pettit.** Biodegradable polymers for protein and peptide drug delivery. *Bioconjug. Chem.* 6: 332–351, 1995.
17. **Ham, A. W.** Some histophysiological problems peculiar to calcified tissues. *J. Bone Joint Surg. Am.* 34A: 701–728, 1952.
18. **Harada, I.** The effects of glucocorticoids on angiogenesis in vitro. *Nippon Seikeigeka Gakkai Zasshi* 66: 763–770, 1992.
19. **Harada, S., J. A. Nagy, K. A. Sullivan, K. A. Thomas, N. Endo, G. A. Rodan, and S. B. Rodan.** Induction of vascular endothelial growth factor expression by prostaglandin E2 and E1 in osteoblasts. *J. Clin. Invest.* 93: 2490–2496, 1994.
20. **Jackson, J., J. Minton, M. Ho, N. Wei, and J. Winkler.** Expression of vascular endothelial growth factor in synovial fibroblasts is induced by hypoxia and interleukin 1-beta. *J. Rheumatol.* 24: 1253–1259, 1997.
21. **Joyce, M. E., S. Jingushi, and M. E. Bolander.** Transforming growth factor-beta in the regulation of fracture repair. *Orthop. Clin. North Am.* 21: 199–209, 1990.
22. **Kueng, W., E. Silber, and U. Eppenberger.** Quantification of cells cultured on 96-well plates. *Anal. Biochem.* 182: 16–19, 1989.
23. **Leung, D. W., G. Cachianes, W. J. Kuang, D. V. Goeddel, and N. Ferrara.** Vascular endothelial growth factor is a secreted angiogenic mitogen. *Science* 246: 1306–1309, 1989.
24. **Lind, M., B. Schumacker, K. Soballe, J. Keller, F. Melsen, and C. Bunger.** Transforming growth factor-beta enhances fracture healing in rabbit tibiae. *Acta Orthop. Scand.* 64: 553–556, 1993.

25. **Linkhart, T. A., S. Mohan, and D. J. Baylink.** Growth factors for bone growth and repair: IGF, TGF-β, and BMP. *Bone* 19: 1S-12S, 1996.
26. **Mandriota, S. J., and M. S. Pepper.** Vascular endothelial growth factor-induced in vitro angiogenesis and plasminogen activator expression are dependent on endogenous basic fibroblast growth factor. *J. Cell Sci.* 110: 2293–2302, 1997.
27. **Passaniti, A., R. M. Taylor, R. Pili, Y. Guo, P. V. Long, J. A. Haney, R. R. Pauly, D. S. Grant, and G. R. Martin.** A simple, quantitative method for assessing angiogenesis and antiangiogenic agents using reconstituted basement membrane, heparin, and fibroblast growth factor. *Lab. Invest.* 67: 519–528, 1992.
28. **Pepper, M. S.** Transforming growth factor-beta: vasculogenesis, angiogenesis, and vessel wall integrity. *Cytokine Growth Factor Rev.* 8: 21–43, 1997.
29. **Pfeilschifter, J., L. Bonewald, and G. R. Mundy.** Characterization of the latent transforming growth factor beta complex in bone. *J. Bone Miner. Res.* 5: 49–58, 1990.
30. **Phillips, G. D., R. A. Whitehead, A. M. Stone, M. W. Ruebel, M. L. Goodkin, and D. R. Knighton.** Transforming growth factor beta (TGF-β) stimulation of angiogenesis: an electron microscopic study. *J. Submicrosc. Cytol. Pathol.* 25: 149–155, 1993.
31. **Robey, P. G., M. F. Young, K. C. Flanders, N. S. Roche, P. Kondaiah, A. H. Heddi, J. D. Termine, M. B. Sporn, and A. B. Roberts.** Osteoblasts synthesize and respond to transforming growth factor-type β (TGF-β) in vitro. *J. Cell Biol.* 106: 457–463, 1987.
32. **Roth, D. A., L. I. Gold, V. K. Han, J. G. McCarthy, J. J. Sung, J. H. Wisoff, and M. T. Longaker.** Immunolocalization of transforming growth factor beta 1, beta 2, and beta 3 and insulin-like growth factor I in premature cranial suture fusion. *Plast. Reconstr. Surg.* 99: 300–309.
33. **Sandberg, M. M., H. T. Aro, and E. I. Vuorio.** Gene expression during bone repair. *Clin. Orthop.* 289: 292–312, 1993.
34. **Shalaby, F., J. Rossant, T. P. Yamaguchi, M. Gertsenstein, X. F. Wu, M. L. Breitman, and A. C. Schuh.** Failure of blood-island formation and vasculogenesis in Flk-1-deficient mice. *Nature* 376: 62–66, 1995.
35. **Shweiki, D., A. Itin, D. Soffer, and E. Keshet.** Vascular endothelial growth factor induced by hypoxia may mediate hypoxia-initiated angiogenesis. *Nature* 359: 843–845, 1992.
36. **Smith, D. W.** Is avascular necrosis of the femoral head the result of inhibition of angiogenesis? *Med. Hypotheses* 49: 497–500, 1997.
37. **Streeten, E. A., and M. L. Brandi.** Biology of bone endothelial cells. *Bone Miner.* 10: 85–94, 1990.
38. **Wang, D. S., K. Yamazaki, K. Nohtomi, K. Shizume, K. Ohsumi, M. Shibuya, H. Demura, and K. Sato.** Increase of vascular endothelial growth factor mRNA expression by 1,25-dihydroxyvitamin D3 in human osteoblast-like cells. *J. Bone Miner. Res.* 11: 472–479, 1996.
39. **Yamamoto, H., H. Ueno, A. Ooshima, and A. Takeshita.** Adenovirus-mediated transfer of a truncated transforming growth factor- beta (TGF-beta) type II receptor completely and specifically abolishes diverse signaling by TGF-beta in vascular wall cells in primary culture. *J. Biol. Chem.* 271: 16253–16259, 1996.
40. **Yang, E. Y., and H. L. Moses.** Transforming growth factor beta 1-induced changes in cell migration, proliferation, and angiogenesis in the chicken chorioallantoic membrane. *J. Cell Biol.* 111: 731–741, 1990.
41. **Yee, J. A., L. Yan, J. C. Dominguez, E. H. Allan, and T. J. Martin.** Plasminogen-dependent activation of latent transforming growth factor beta (TGF beta) by growing cultures of osteoblast-like cells. *J. Cell. Physiol.* 157: 528–534, 1993.